NADPH absorbance at 340 nm), which was inhibited by 2-deoxyglucose. However, GPA could not inhibit this increase in hexokinase activity, indicating that GPA was not a hexokinase inhibitor. Error bars: standard deviation (n = 3).

(**B**) Inhibition of glucose uptake by GPA. GPA inhibited the uptake of the glucose-mimic 2-deoxyglucose (2DG) in a dose dependent manner. Error bars: standard deviation (n = 3). Similar results were obtained from three individual experiments. These results explain the glucose-6-phosphate decrease depicted in **Figure 4**.

(**C**) Inhibition of GLUT1-mediated glucose uptake by GPA. Since glucose uptake in A431 cells is primarily mediated by GLUT1, A431 GLUT1 was overexpressed, and the sensitivity of glucose uptake to GPA was examined. Overexpression lowered the sensitivity 2DG uptake inhibition by GPA as observed with the shift of the inhibition curve to the right. Error bars: standard deviation (n = 3). The data shown represent results of three independent experiments.

(See also **Fig S5**.)

Table 1: Inhibitory activities of remixing silica gel chromatography fractions, and the effect of withholding each fraction from the Remix.

(See **Fig S1** for the bioassay-guided isolation of the compounds.)

sample #	fractions eluted with $CHCl_3$: MeOH						Filopodia Protrusion
	100 : 0 **I**	100 : 1 **II**	100 : 2 **III**	100 : 5 **IV**	100 : 10 **V**	100 : 30 **VI**	
Remix	contained	contained	contained	contained	contained	contained	Inhibition
Remix – **I**		contained	contained	contained	contained	contained	***No inhibition***
Remix – **II**	contained		contained	contained	contained	contained	Inhibition
Remix – **III**	contained	contained		contained	contained	contained	Inhibition
Remix – **IV**	contained	contained	contained		contained	contained	***No inhibition***
Remix – **V**	contained	contained	contained	contained		contained	Inhibition
Remix – **VI**	contained	contained	contained	contained	contained		Inhibition
I + IV	contained			contained			***Inhibition***
I	contained						No inhibition
IV				contained			No inhibition

Figure 1

A

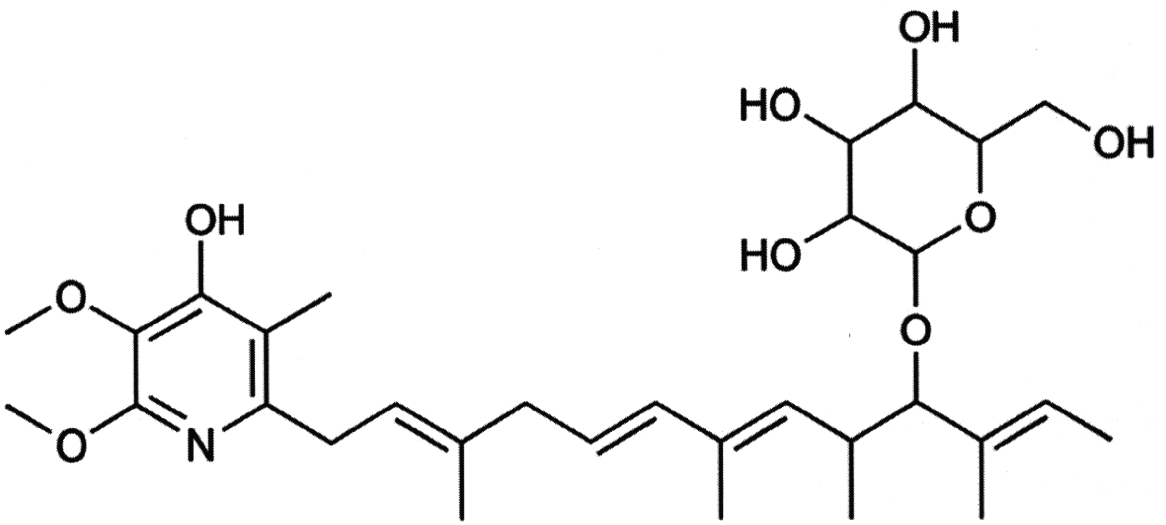

glucopiericidin A

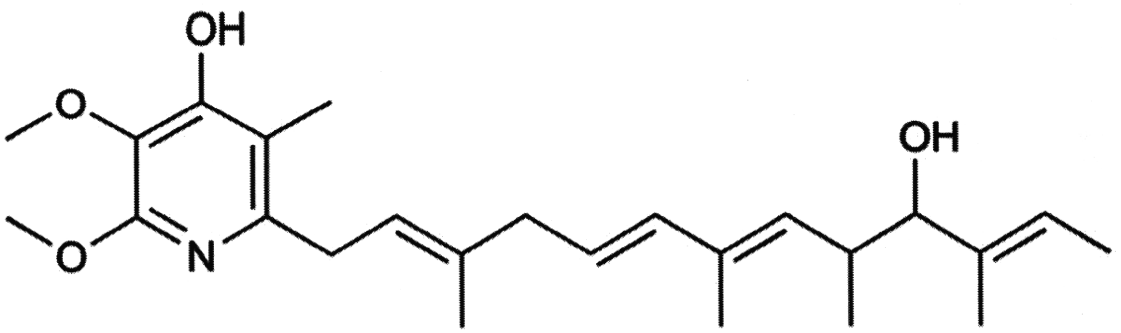

piericidin A

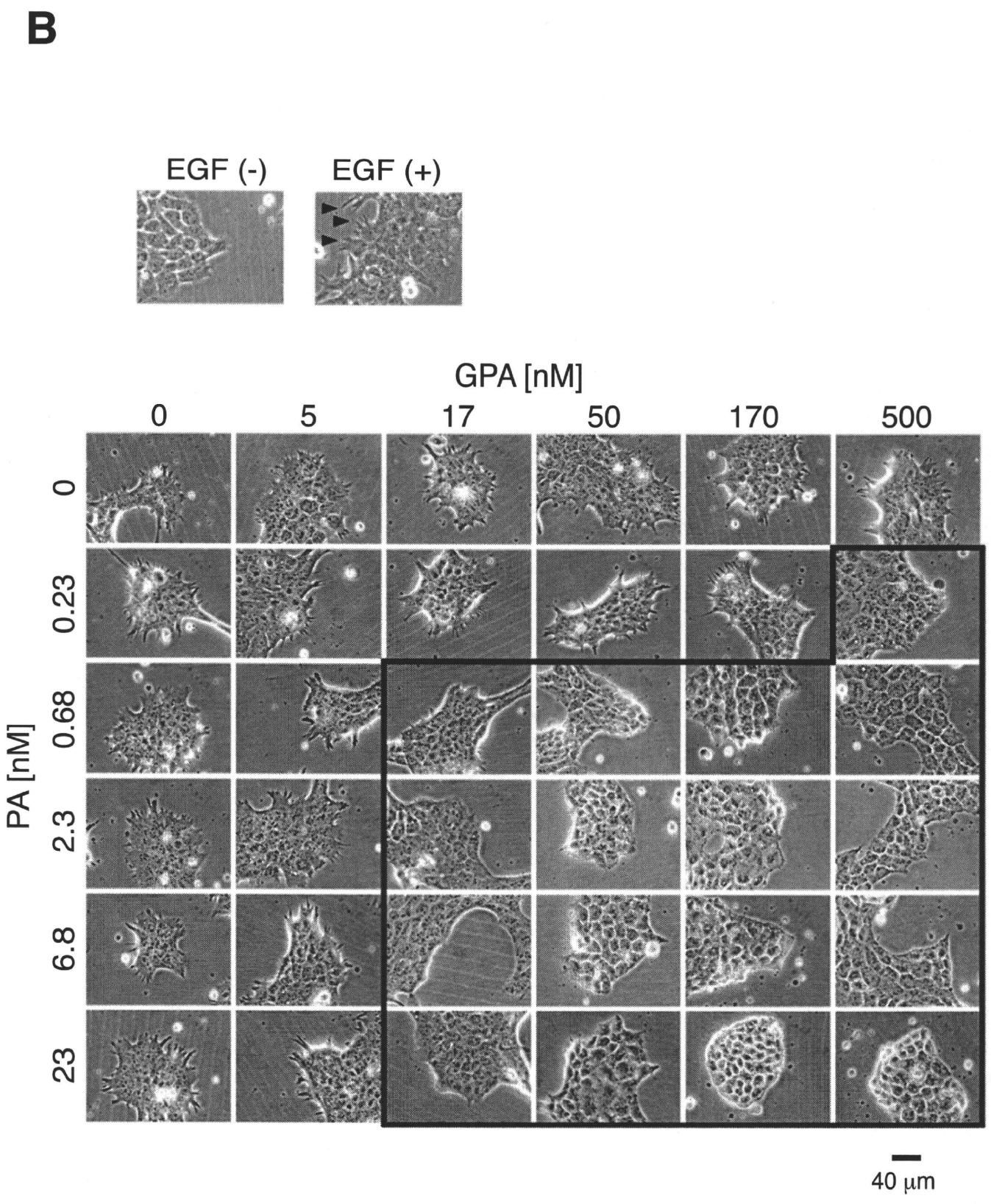
B
EGF (-)
EGF (+)
GPA [nM]
0
5
17
50
170
500
PA [nM]
0
0.23
0.68
2.3
6.8
23
40 μm

C

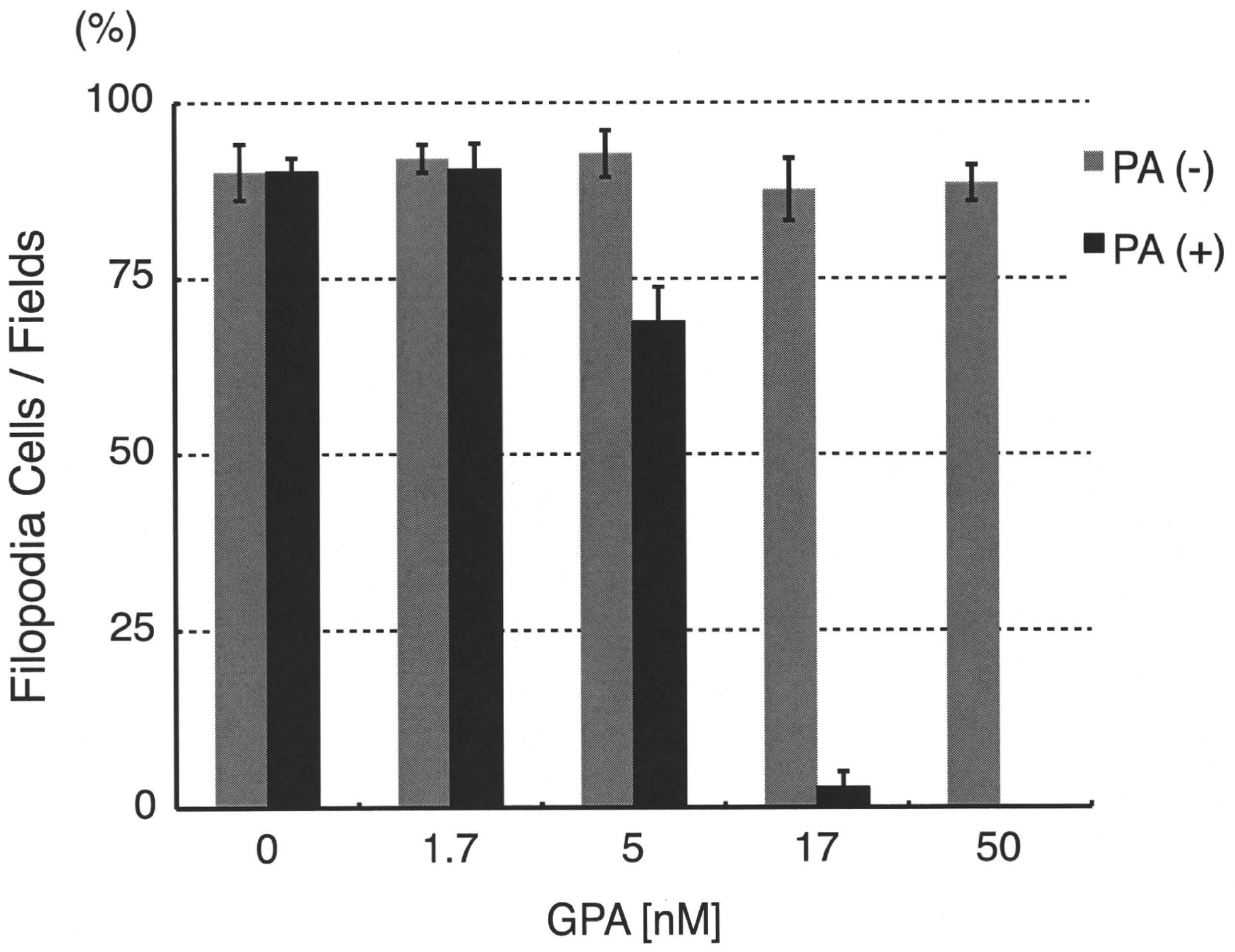

Figure 2

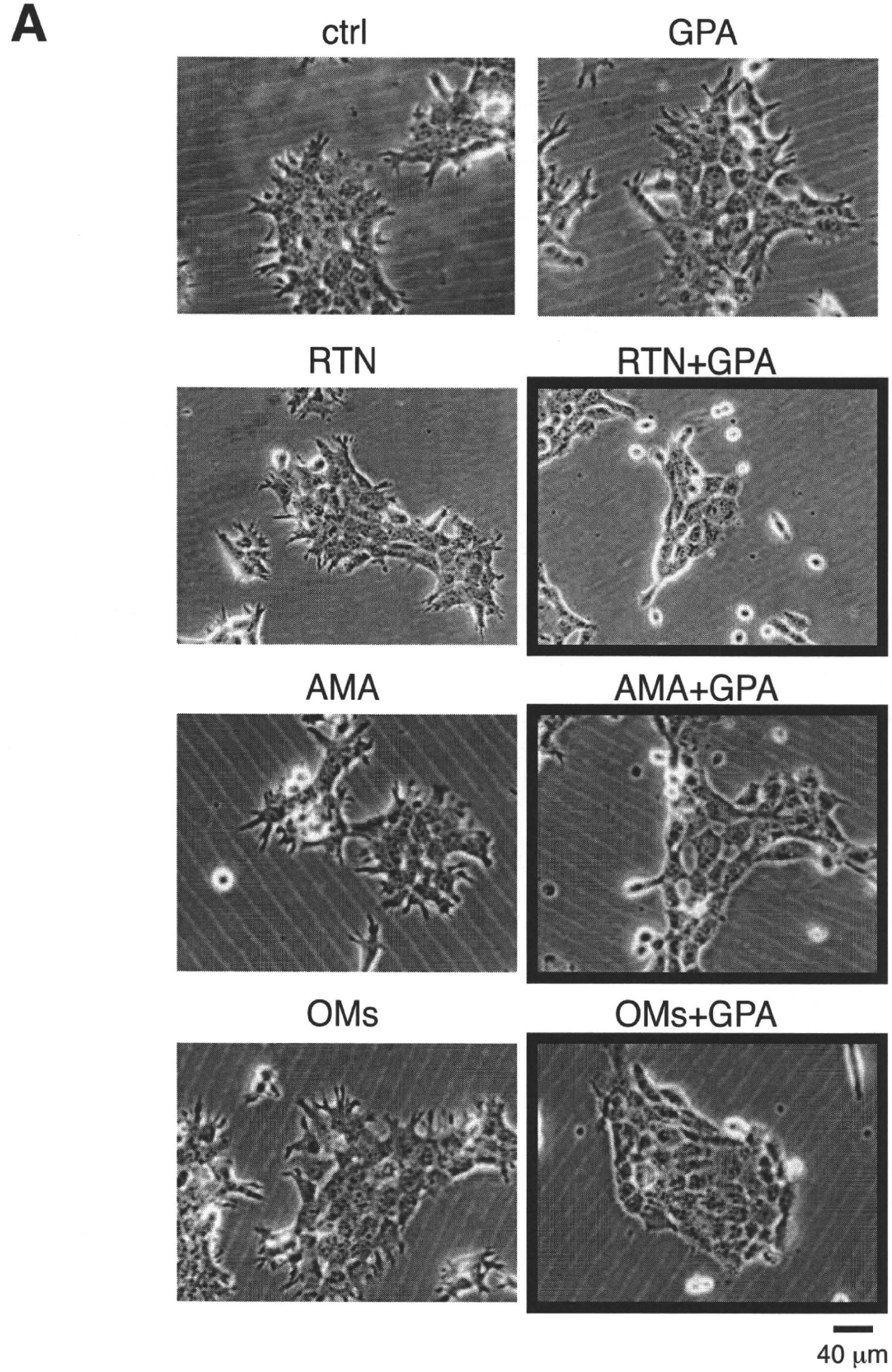

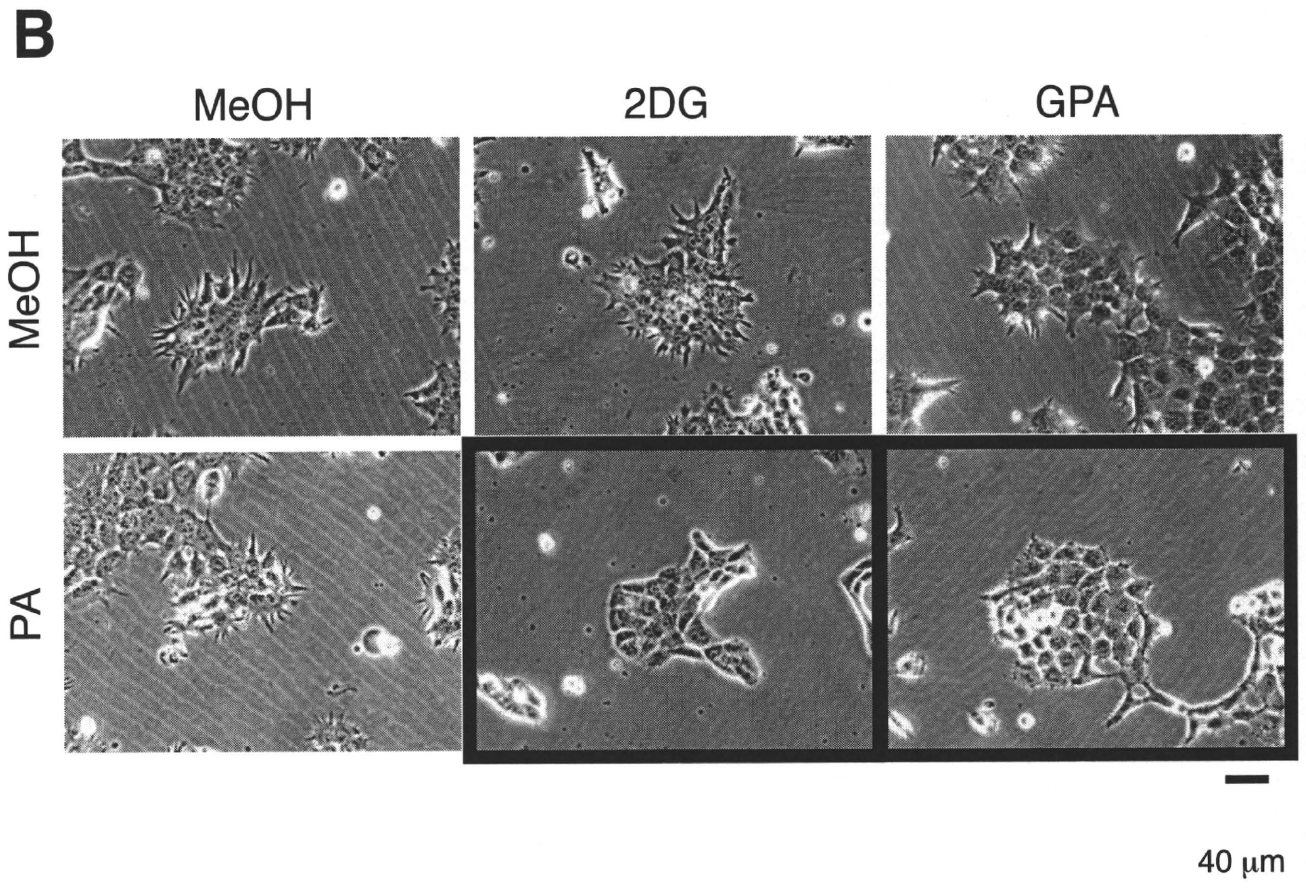
B
MeOH
2DG
GPA
MeOH
PA
40 μm

C

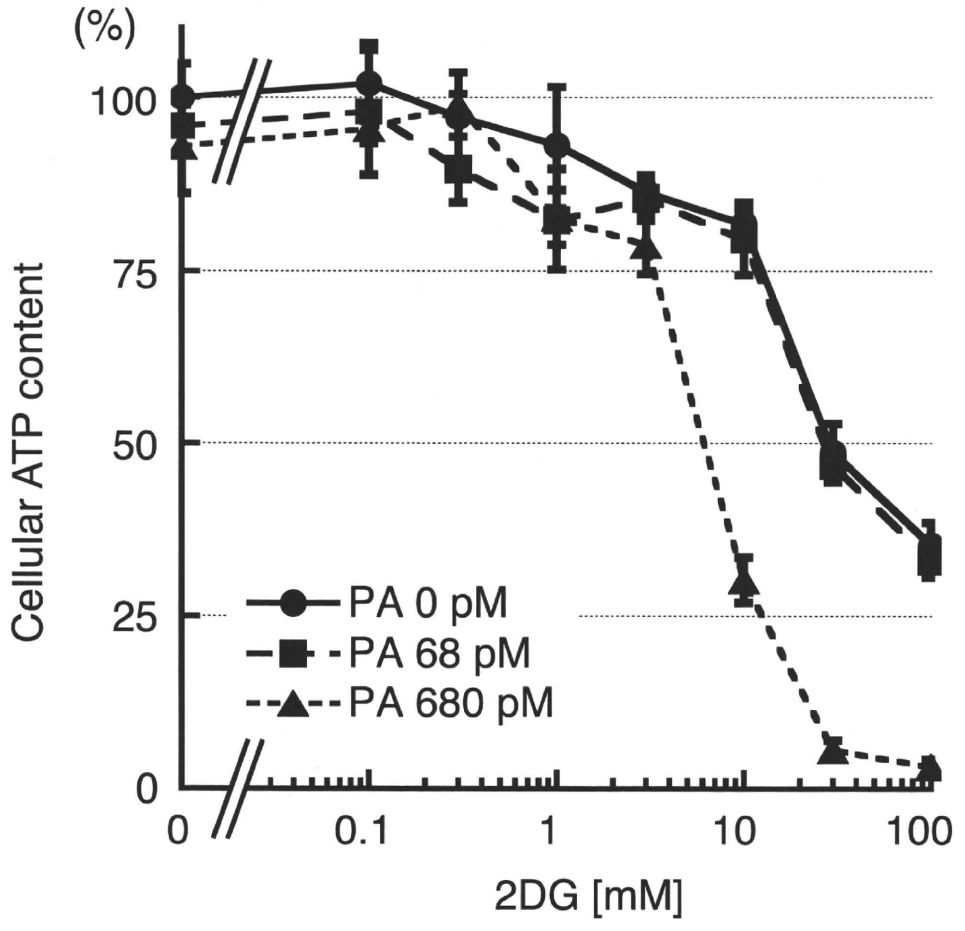
(%)
100
75
50
25
0
Cellular ATP content
PA 0 pM
PA 68 pM
PA 680 pM
0
0.1
1
10
100
2DG [mM]

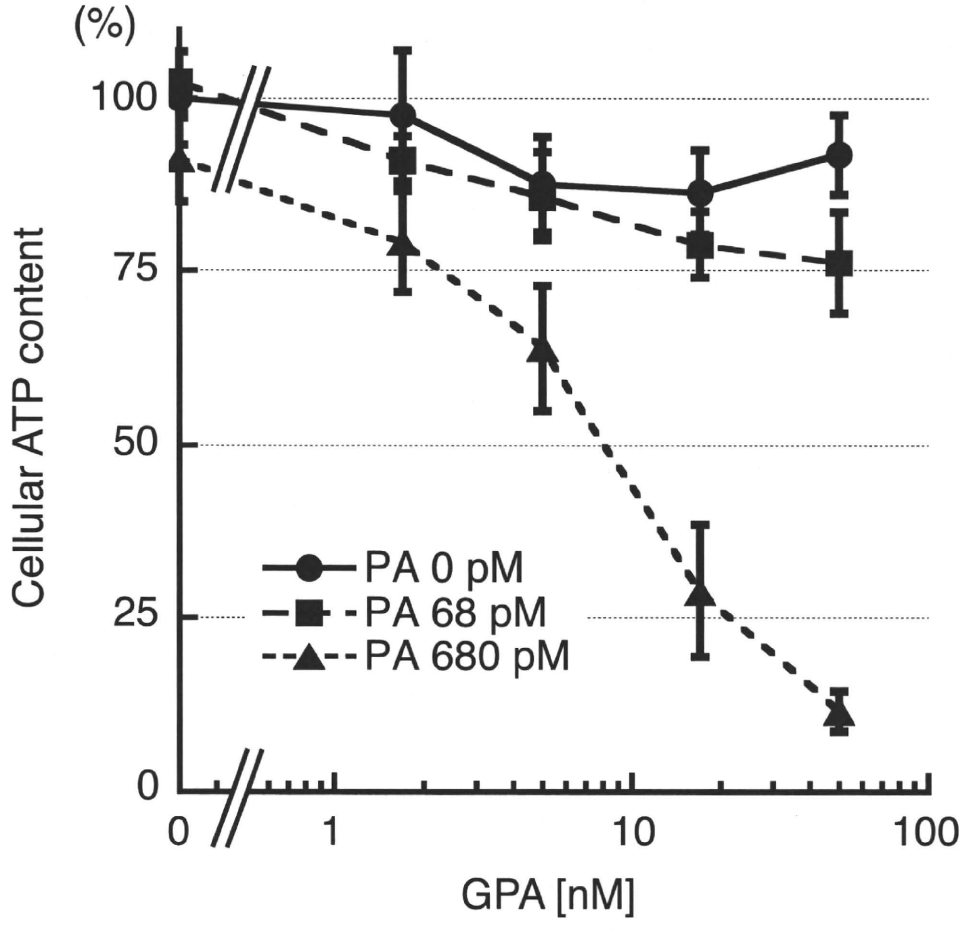
(%)
100
75
50
25
0
Cellular ATP content
PA 0 pM
PA 68 pM
PA 680 pM
0
1
10
100
GPA [nM]

Figure 3

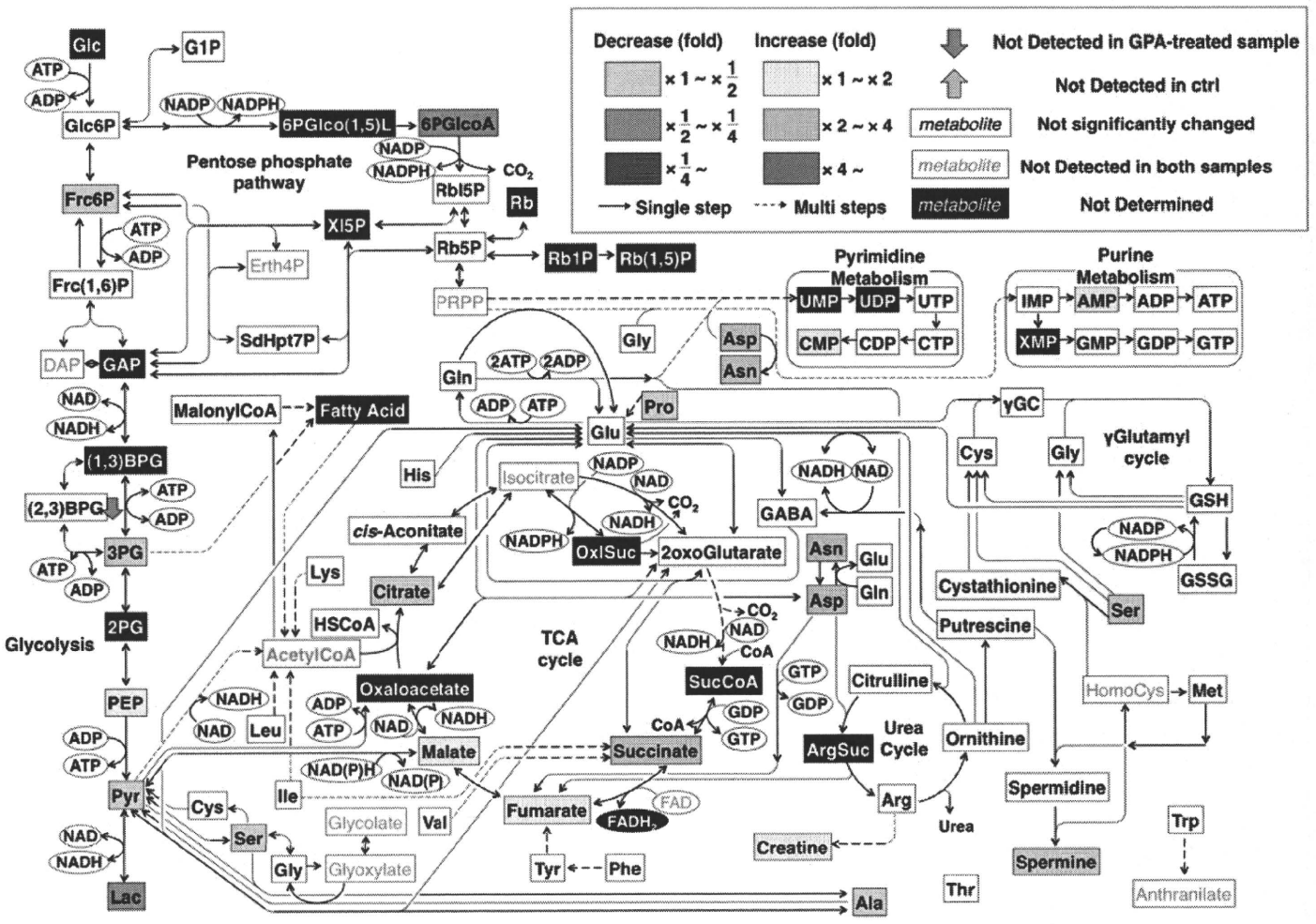
Decrease (fold)
Increase (fold)
Not Detected in GPA-treated sample
Not Detected in ctrl
Not significantly changed
Not Detected in both samples
Not Determined
Single step
Multi steps
Glc
G1P
Glc6P
6PGlco(1,5)L
6PGlcoA
Pentose phosphate pathway
Rbl5P
Frc6P
Xl5P
Rb5P
Rb1P
Rb(1,5)P
Erth4P
SdHpt7P
Frc(1,6)P
DAP
GAP
PRPP
Pyrimidine Metabolism
Purine Metabolism
UMP
UDP
UTP
CMP
CDP
CTP
IMP
AMP
ADP
ATP
XMP
GMP
GDP
GTP
Gly
Asp
Asn
Gln
Pro
Glu
MalonylCoA
Fatty Acid
(1,3)BPG
(2,3)BPG
3PG
2PG
PEP
Pyr
Lac
Glycolysis
His
Isocitrate
cis-Aconitate
Citrate
Lys
HSCoA
AcetylCoA
Oxaloacetate
Malate
Leu
Ile
Cys
Ser
Glycolate
Val
Glyoxylate
TCA cycle
OxlSuc
2oxoGlutarate
SucCoA
Succinate
Fumarate
FADH2
FAD
Tyr
Phe
Ala
GABA
Asn
Glu
Gln
Asp
Citrulline
ArgSuc
Urea Cycle
Arg
Urea
Ornithine
Creatine
Thr
yGC
Cys
Gly
yGlutamyl cycle
GSH
GSSG
Cystathionine
Ser
Putrescine
HomoCys
Met
Spermidine
Spermine
Trp
Anthranilate

Figure 4

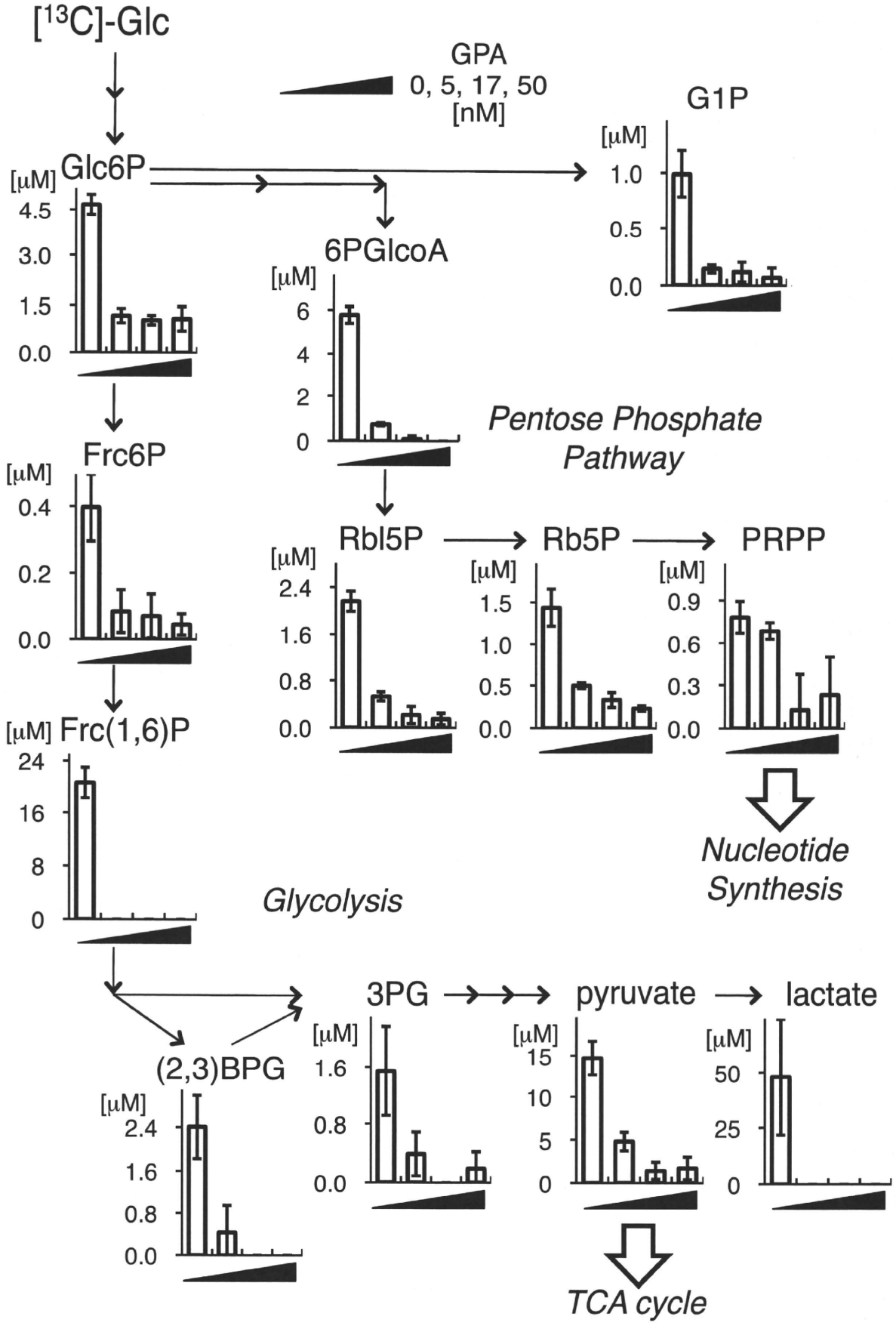
[13C]-Glc
GPA
0, 5, 17, 50
[nM]
G1P
[μM]
1.0
0.5
0.0
Glc6P
[μM]
4.5
3.0
1.5
0.0
6PGlcoA
[μM]
6
4
2
0
Pentose Phosphate
Pathway
Frc6P
[μM]
0.4
0.2
0.0
Rbl5P
Rb5P
PRPP
[μM]
2.4
1.6
0.8
0.0
[μM]
1.5
1.0
0.5
0.0
[μM]
0.9
0.6
0.3
0.0
Nucleotide
Synthesis
[μM] Frc(1,6)P
24
16
8
0
Glycolysis
3PG
pyruvate
lactate
(2,3)BPG
[μM]
2.4
1.6
0.8
0.0
[μM]
1.6
0.8
0.0
[μM]
15
10
5
0
[μM]
50
25
0
TCA cycle

Figure 5

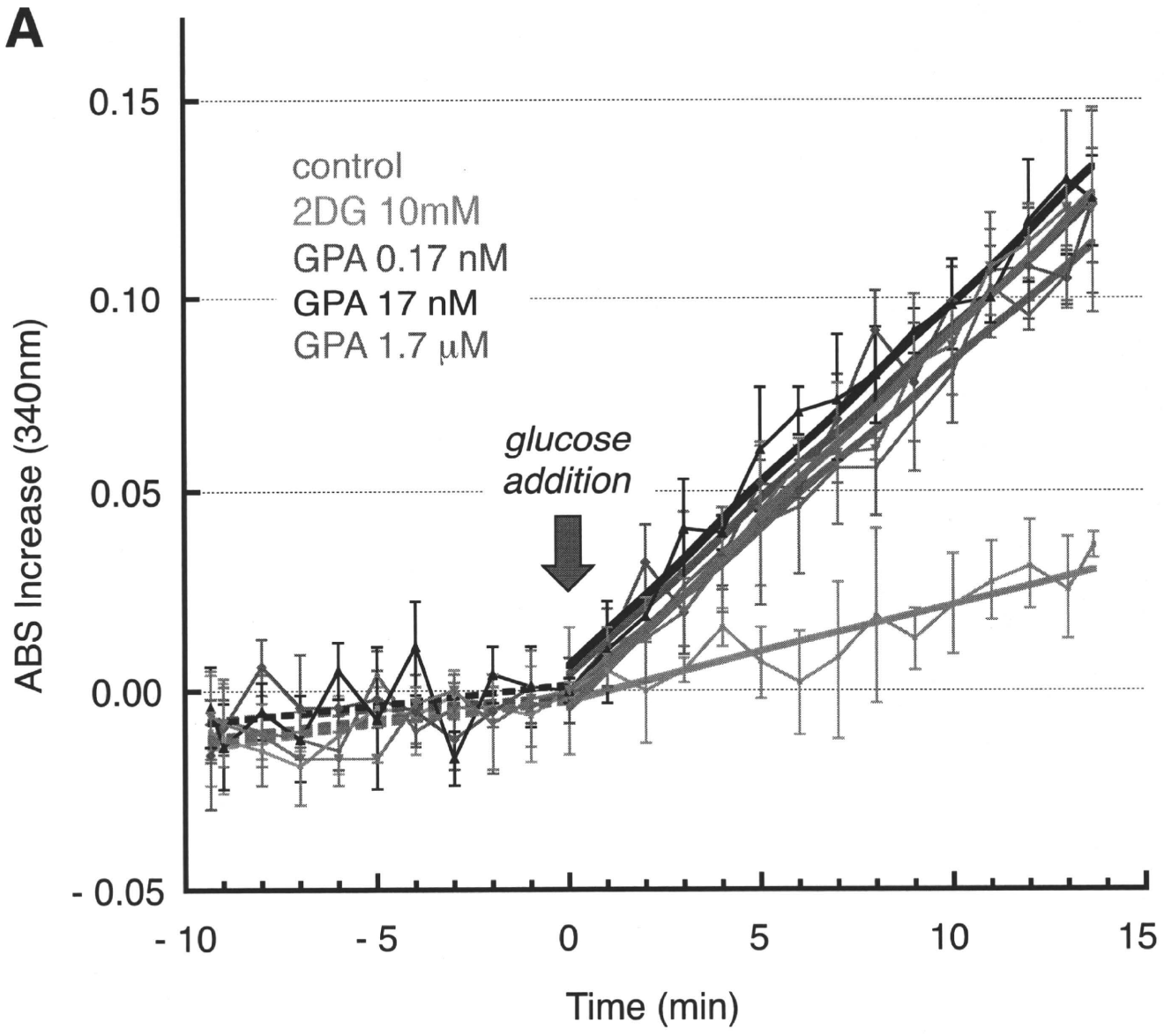
A
0.15
0.10
0.05
0.00
- 0.05
ABS Increase (340nm)
control
2DG 10mM
GPA 0.17 nM
GPA 17 nM
GPA 1.7 μM
glucose
addition
- 10
- 5
0
5
10
15
Time (min)

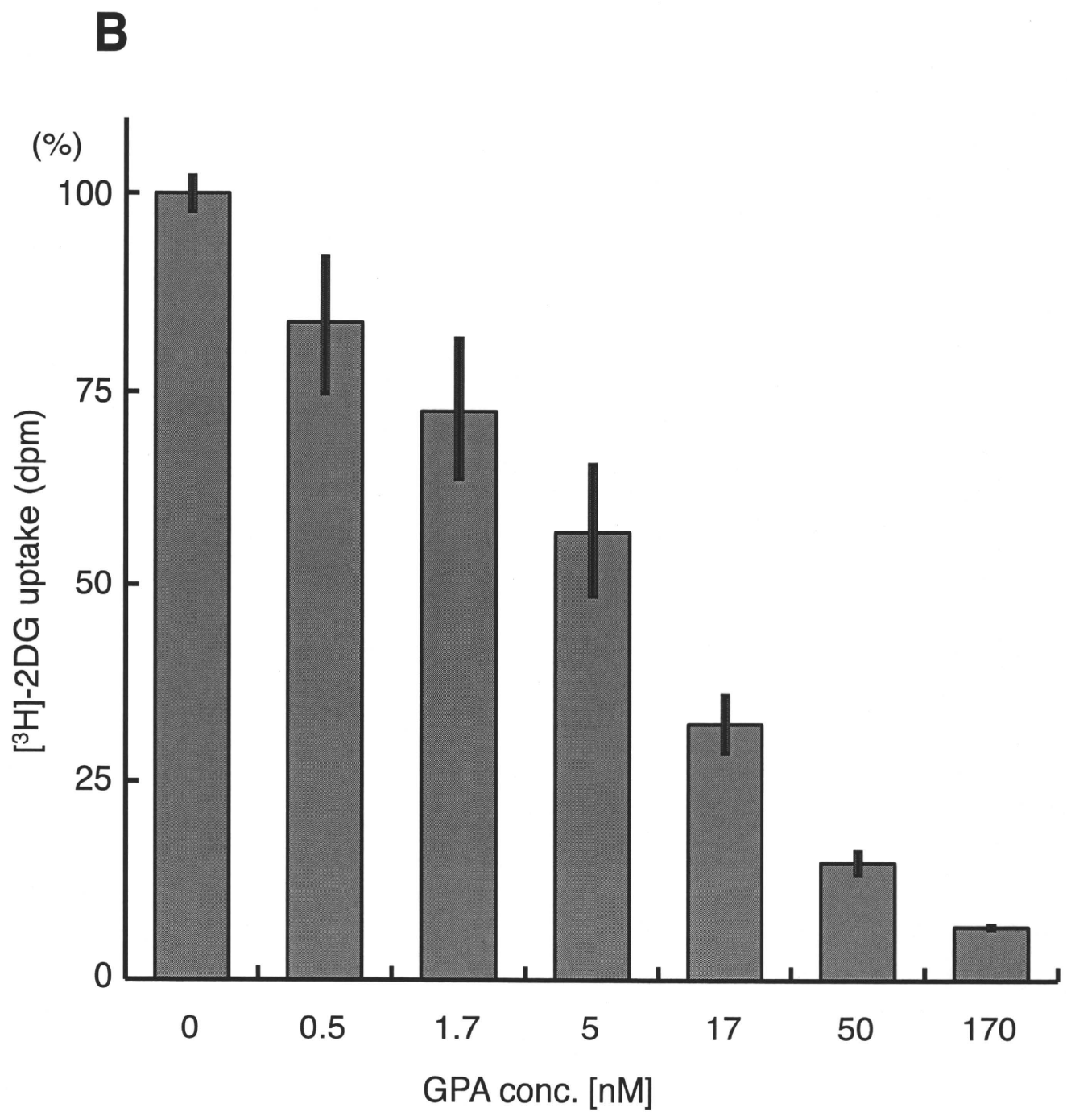
B
(%)
100
75
50
25
0
[3H]-2DG uptake (dpm)
0
0.5
1.7
5
17
50
170
GPA conc. [nM]

C

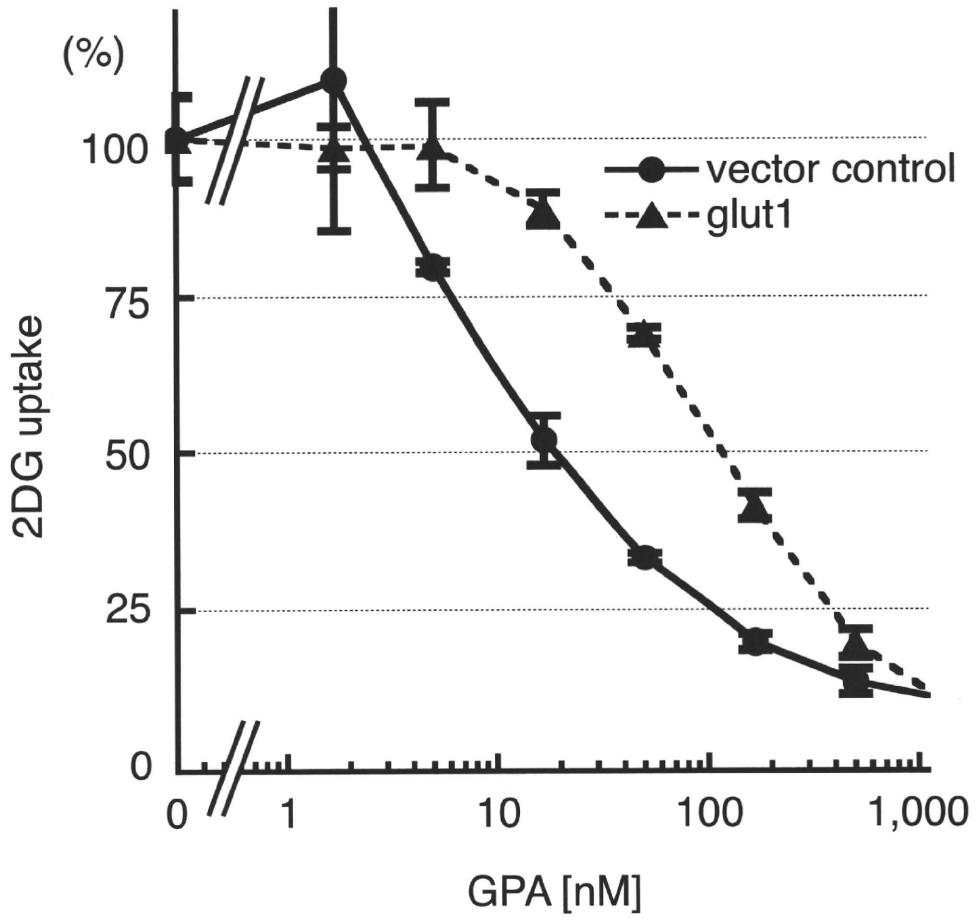
(%)
100
75
50
25
0
2DG uptake
vector control
glut1
0
1
10
100
1,000
GPA [nM]

Connections of each supplemental data to the main data

Figure S1, Bioassay-guided isolation of the filopodia inhibitor from microbial broth, related to **Figure 1** and **Table 1**. It provides the evidence of the process for the compounds isolation shown in **Figure 1A** (**Fig S1A-E**) and supports compounds activity in **Figure 1B** and **C** (**Fig S1F**).

Table S1, Assignments of 13C- and 1H-NMR of glucopiericidin A (GPA) and piericidin A (PA), related to **Figure 1**. It assigns the structures of the isolated compounds shown in **Figure 1A**.

Figure S2, Inhibitory activity against mitochondrial NADH oxidase, related to **Figure 2**. It provides the reason why the article discussed about the target protein and mode of action of GPA for further as a main question.

Table S2, Compounds for chemical genomic screening, related to **Figure 2**. According to this result, we did the experiments shown in **Figure 2B** and **C**.

Figure S3, Decrease of lac/pyr ratio by GPA, related to **Figure 3**. It supports the novel mode of action of GPA described in the main text.

Table S3, Metabolite levels in control and GPA-treated cells, related to **Figure 3**. It is the entire result of whole metabolome analysis shown in **Figure 3**.

Figure S4 does not exist.

Table S4, Isotopomers detected in analysis of [13C]-glucose metabolism, related to **Figure 4**. It is the entire result of isotope-labeling study shown in **Figure 4**.

Figure S5, Inhibition of glucose uptake by GPA, related to **Figure 5**. It supports the conclusion of the article.

Supplemental Figs Tables Text

Supplemental Information

Metabolomic identification of the target of the filopodia protrusion inhibitor glucopiericidin A

Mitsuhiro Kitagawa, Satsuki Ikeda, Etsu Tashiro, Tomoyoshi Soga & Masaya Imoto*

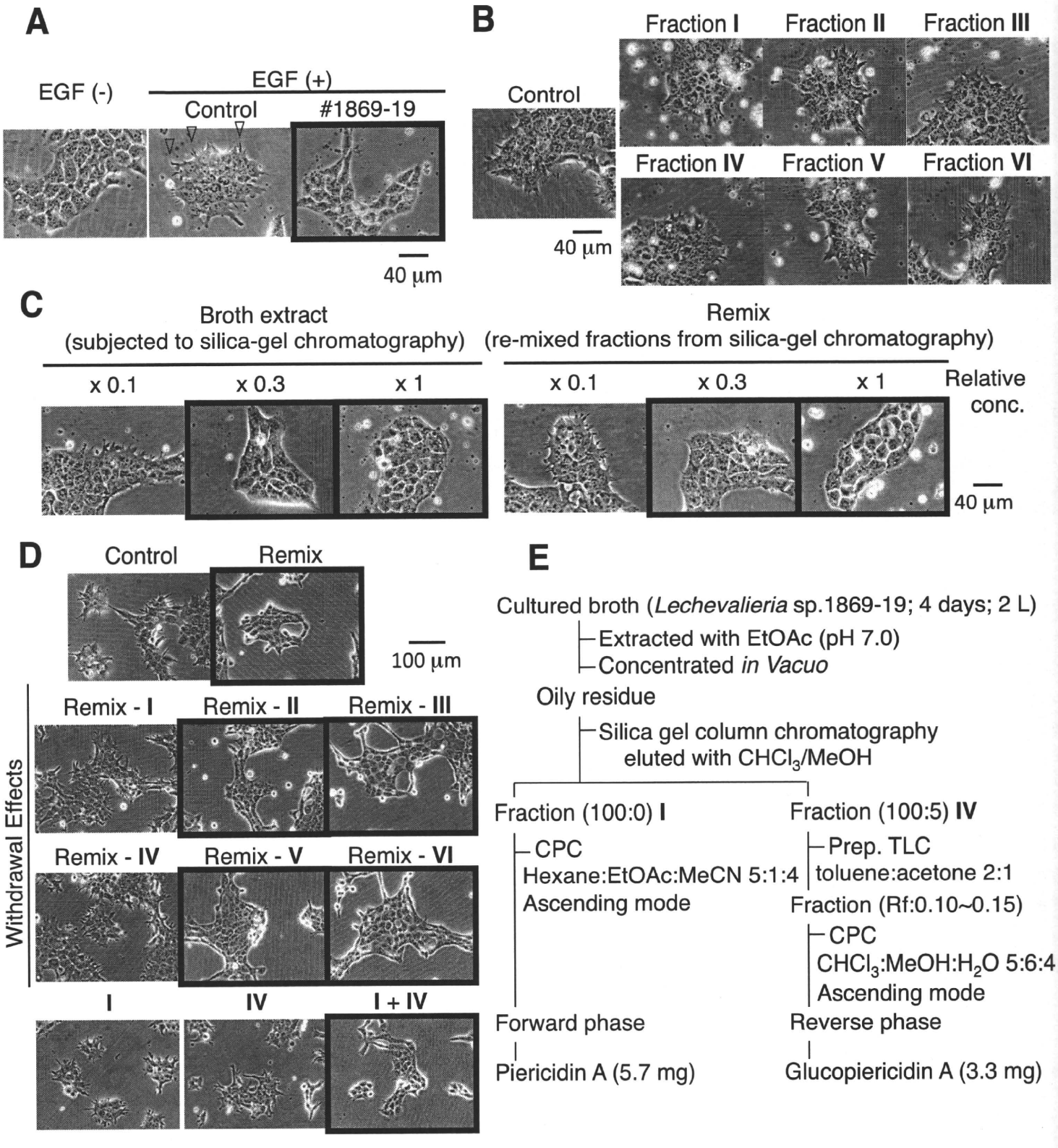

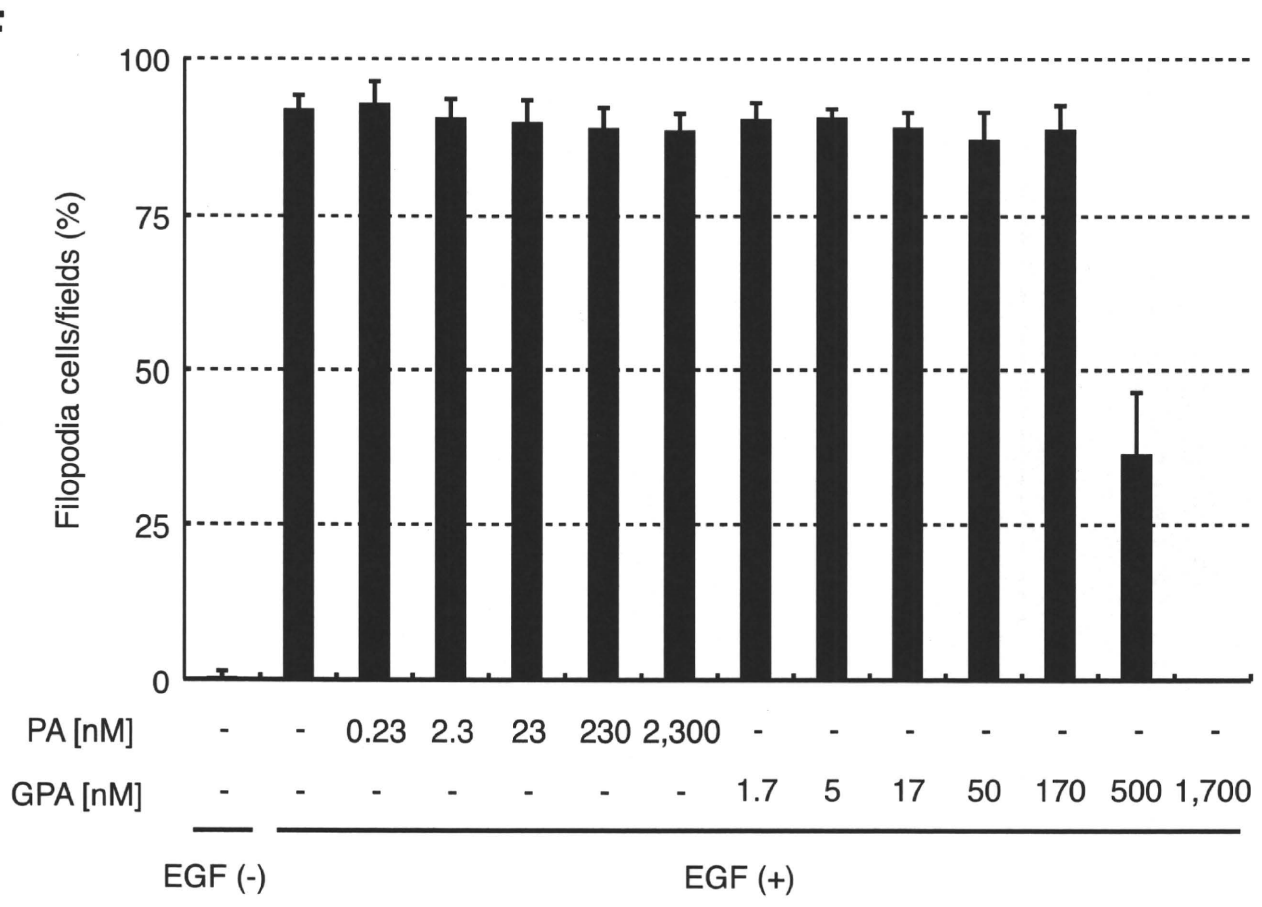

Figure S1, related to Figure 1: Bioassay-guided isolation of the filopodia inhibitor from microbial broths.

(**A**) The result of screening for the filopodia inhibitor. A431 cells stimulated with EGF (30 ng ml^{-1}) protruded sting-formed filopodia (arrow head), but these were completely inhibited by the broth extract of *Lechevalieria* sp. strain #1869-19, indicating that this broth contained the filopodia inhibitor.

(**B**, **C**, **D**) The cooperative filopodia inhibition caused by two or more components in the broth. Any single fractions eluted from silica gel column chromatography did not inhibit the filopodia (**B**), but when they were mixed together again ("Remix"), filopodia protrusion was inhibited in the same concentration range as the broth extract (**C**), indicating that the inhibitory activity of the broth extract was due to synergy between two or more broth components, which was fractionated into the different fractions with each other. Moreover, when fraction **I** or **IV** was withdrawn from "Remix", the inhibition was not observed, indicating that these synergistic broth components were fractionated in **I** and **IV** (**D**, see also **Table 1**).

(**E**) Purification procedure of piericidin A and glucopiericidin A.

(**F**) Weak activity of GPA and inactivity of PA on filopodia protrusion inhibition in a single treatment. The number of colonies of filopodia-positive cells were counted by microscopy, and the rate of formation [filopodia colonies] / [total colonies] was calculated. Error bars represent standard deviation (n = 9).

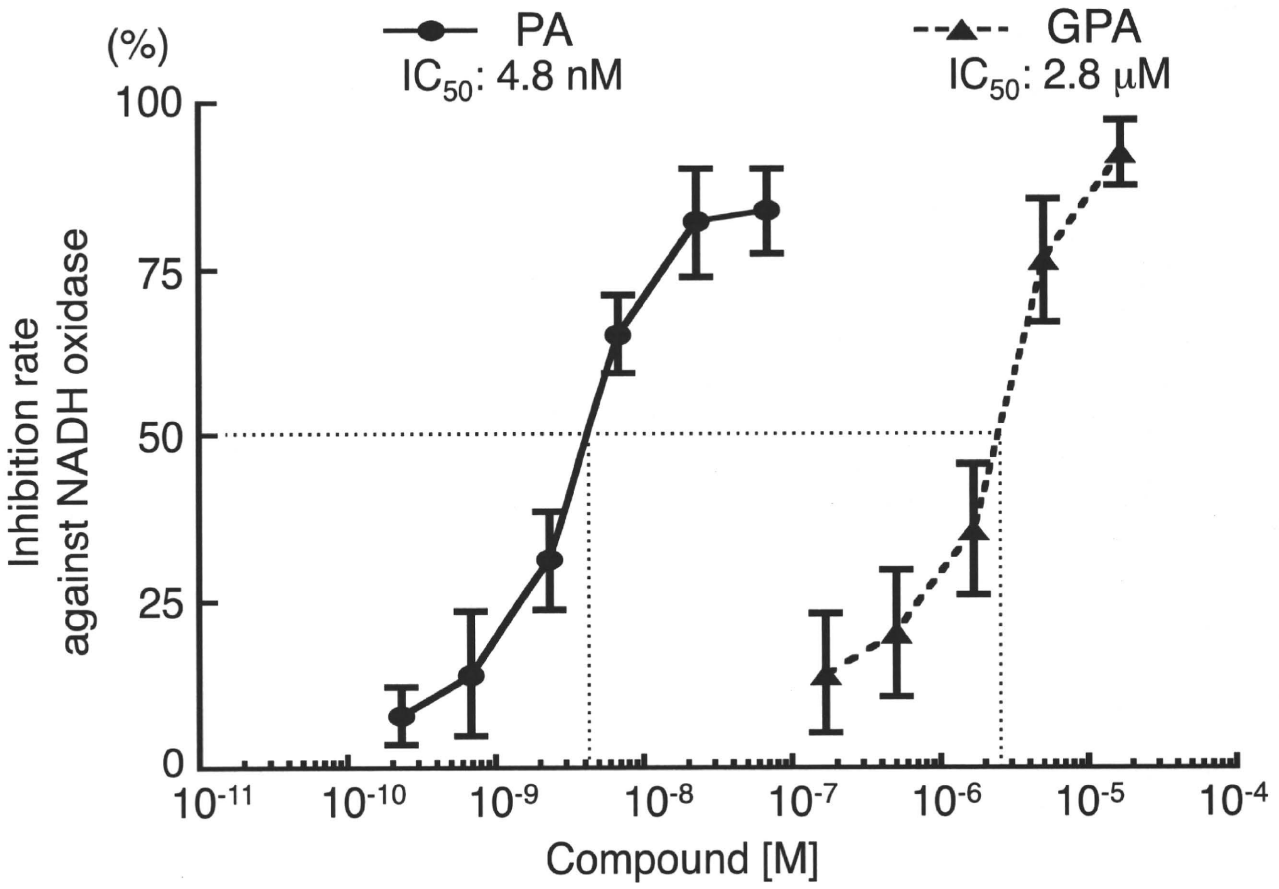

Figure S2, related to Figure 2: Inhibitory activity against mitochondrial NADH oxidase.

As described in **Experimental Procedures**, inhibitory activity of PA and GPA against mitochondrial NADH oxidase activity *in vitro* was determined. Inhibitory activity of GPA was quite low (IC_{50} value: 2.8 μM), while structurally related PA showed strong inhibition (IC_{50} value: 4.8 nM). Error bars: standard deviation. (n = 4).

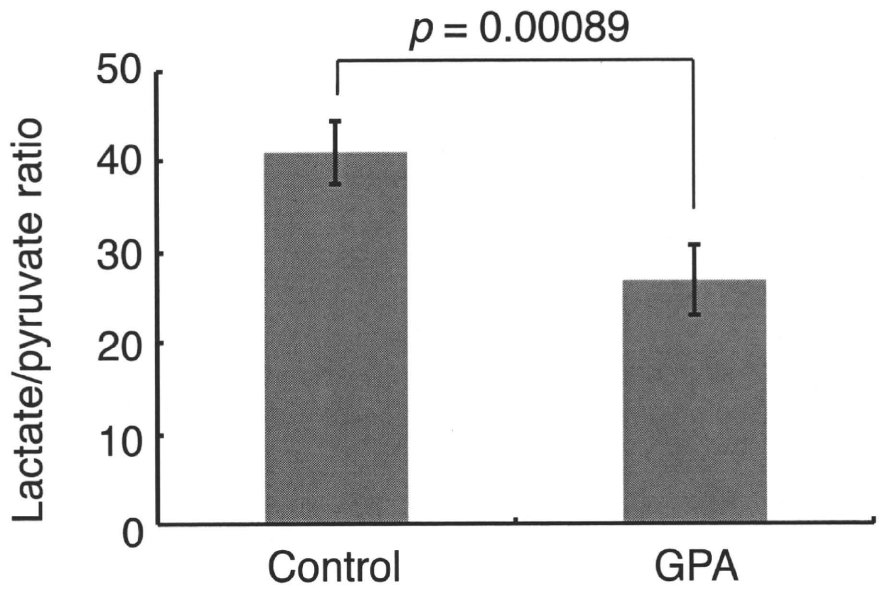

Figure S3, related to Figure 3 and Table S3: Decrease of lac/pyr ratio by GPA.

GPA decreased the end-products levels of glycolysis in cells (**Figure 3** and **Table S3**). The ratio of lactate/pyruvate levels, another glycolytic parameter, also decreased significantly, supporting the conclusion that GPA inhibits glycolysis. Error bars: standard deviation (n = 4).

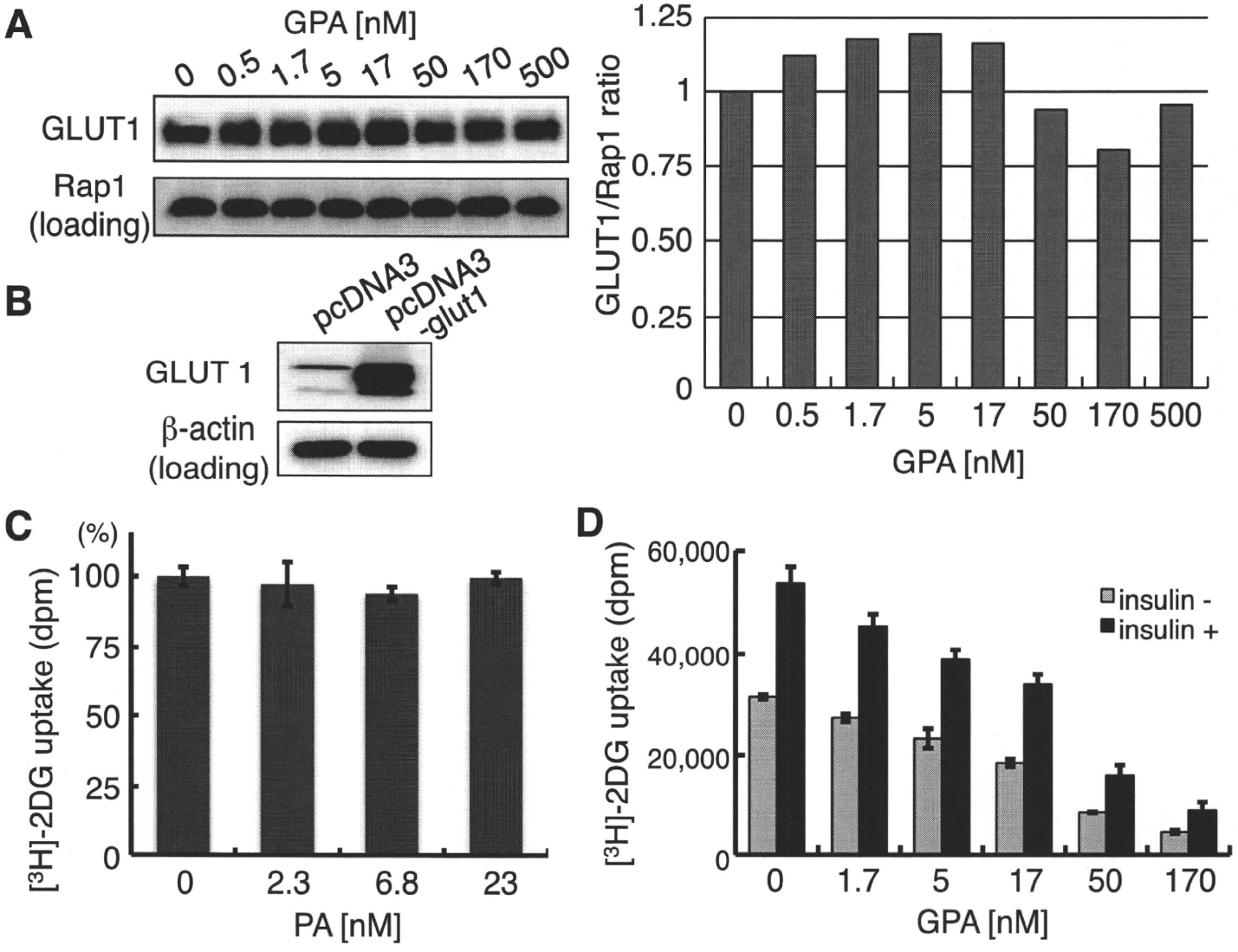

Figure S5, related to Figure 5: Inhibition of glucose uptake by GPA.

(**A**) No change in the GLUT1 expression level in plasma membrane in GPA-treated cells. To distinguish whether the glucose uptake inhibition by GPA shown in **Figure 5B** was made by either the functional inhibition of GLUT, or the changes in GLUT expression level, the latter was examined by immunoblotting. Since it was reported that GLUT1 accounts for the major part of glucose uptake in A431 cells (Aloj, et al., 1999) and was in plasma membrane, the GLUT1 expression level in the plasma membrane was examined as described in **Supplemental Experimental Procedures**. Rap1 was the loading control of cell membrane fraction. Quantification of each band (right) was done by ImageJ. The expression level in plasma membrane was not much changed by GPA treatment, indicating that GPA would inhibit GLUT function.

(**B**) Expression level of GLUT 1 in HEK293T cells in **Figure 5C**.

(**C**) Importance of the glucopyranoside moiety in the GPA structure for glucose uptake inhibition. As shown here, glucose uptake could not be inhibited by PA, which lacks the glucopyranoside moiety. This indicates that the glucopyranoside moiety of GPA is important for the inhibitory activity of GPA to glucose uptake, perhaps because the glucopyranoside moiety may mimic the GLUT substrate glucose. Error bas: standard deviation (n = 3).

(**D**) Inhibition of GLUT4-mediated glucose uptake by GPA. To examine the inhibitory activity of GPA on other glucose uptake mediated by GLUTs other than GLUT1, GLUT4 in insulin-stimulated Swiss 3T3 adipocytes was chosen. As previously described, insulin stimulation increased the 2DG uptake in cells, which represents the GLUT4-mediated uptake. This was also inhibited by GPA, indicating that GPA would be able to inhibit GLUT4, too. Error bars: standard deviation (n = 3).

Table S1, related to Figure 1: Assignments of 13C- and 1H-NMR of glucopiericidin A (GPA) and piericidin A (PA).

position	GPA		PA	
	13C	1H	13C	1H
1	34.8 (t)	3.36 (2H, d, 6.9Hz)	34.4	3.37 (2H, d, 7.6Hz)
2	122.5 (d)	5.38 (1H, t, 6.9Hz)	122.2	5.41 (1H, t, 7,6Hz)
3	135.1 (s)		135.6	
4	43.4 (t)	2.77 (2H, d, 7.0Hz)	43.1	2.79 (2H, d, 6.8Hz)
5	127.4 (d)	5.61 (1H, dt, 15.4, 7.0Hz)	126.8	5.61 (1H, dt, 15.8, 6.9Hz)
6	135.5 (d)	6.05 (1H, d, 15.4Hz)	135.7	6.09 (1H, d, 15.8Hz)
7	134.9 (s)		134.8	
8	135.0 (d)	5.23 (1H, d, 9.5Hz)	133.1	5.21 (1H, d, 9.8Hz)
9	35.4 (d)	2.77 (1H, m)	36.9	2.69 (1H, m)
10	95.0 (d)	3.43 (1H, d, 9.7Hz)	82.8	3.62 (1H, d, 9.2Hz)
11	135.9 (s)		136.0	
12	123.9 (d)	5.42 (1H, q, 6.0Hz)	123.6	5.49 (1H, m)
13	13.7 (q)	1.62 (3H, d, 6.0Hz)	13.1	1.63 (3H, d, 6.6Hz)
14	11.2 (q)	1.61 (3H, s)	10.5	1.64 (3H, s)
15	17.2 (q)	0.75 (3H, d, 6.9Hz)	17.4	0.81 (3H, d, 7.2Hz)
16	17.0 (q)	1.78 (3H, s)	16.6	1.75 (3H, s)
17	13.4 (q)	1.74 (3H, s)	13.2	1.81 (3H, s)
1'	151.2 (s)		150.8	
2'	112.4 (s)		112.0	
3'	154.3 (s)		154.0	
4'	128.2 (s)		127.8	
5'	153.9 (s)		153.5	
6'	10.8 (q)	2.08 (3H, s)	10.5	1.64 (3H, s)
7'	61.0 (q)	3.85 (3H, s)	60.6	3.86 (3H, s)
8'	53.5 (q)	3.95 (3H, s)	53.1	3.95 (3H, s)
1"	104.2 (d)	4.14 (1H, d, 7.9Hz)		
2"	74.7 (d)	3.23 (1H, dd, 8.9, 7.9Hz)		
3"	75.6 (d)	3.48 (1H, dd, 8.9, 9.2Hz)		
4"	71.3 (d)	3.43 (1H, t, 9.2Hz)		
5"	76.7 (d)	3.28 (1H, ddd, 3.3, 6.4, 9.2Hz)		
6"	63.2 (t)	3.64 (1H, dd, 6.4, 11,5Hz), 3.81 (1H, dd, 3.3, 11.5Hz)		

Measured in $CDCl_3$

Table S2, related to Figure 2: Compounds for chemical genomic screening.

The inhibition of filopodia protrusion in the absence ("single") or the presence of mitochondrial respiratory inhibitor ("with MRI*") are shown.

Hit criteria: The compound with smaller EC_{100} value "with MRI*" than in a "single" treatment.

Compound		EC_{100}		
name	category	single	with MRI*	
5-FU	thymidylate synthetase	-	-	
Bestatin	aminopeptidase B	-	-	
Bleomycin sulfate	DNA	-	-	
Cisplatin	DNA	-	-	
Methotrexate	DHFR	-	-	
Mitomycin C	DNA	-	-	
Flutamide	AR	-	-	
Daunorubicin, HCl	DNA	-	-	
Doxorubicin, HCl	DNA	-	-	
Tamoxifen, citrate	ER	-	-	
Vinblastin	tublin polymerization	-	-	
Camptothecin	topo I	-	-	
Aclarubicin	topo I/II	-	-	
Etoposide (VP-16)	topo II	-	-	
2',5'-dideoxyadenosine	adenylcyclase	-	-	
AKT inhibitor	AKT	-	-	
NL-71-101	AKT	-	-	
AG957	Bcr-Abl	-	-	
KN93	CAMKII	-	-	
Z-VAD-FMK	caspase	-	-	
Kenpaullone	CDC2	-	-	
Purvalanol A	CDK2	-	-	
3-ATA	CDK4	-	-	
Olomoucine	CDKs	-	-	
TBB	CKII	-	-	
Sulindac sulfide	COX-1	-	-	
Valeryl salicylate	COX-1	-	-	
NS-398	COX-2	-	-	
Theophylline	cyclicphosphodiesterase	-	-	
Azacytidine	DNA methyltransferase	-	-	
Aphidicolin	DNA polymerase	-	-	
AG1478	EGFR	0.1 μM	0.1 μM	
Genistein	EGFR, topoII	-	-	
SU5402	FGFR	-	-	
SU9518	PDGFR	-	-	
Manumycin A	farnesyltransferase	-	-	
SU1498	Flk-1	-	-	
GGTI-286	GGTase I	-	-	
Dexamethasone	GR	-	-	
GSK-3 inhibitor II	GSK-3	-	-	
SB 415286	GSK-3	-	-	
LiCl	GSK-3	-	-	
Scriptaid	HDAC	-	-	
Trichostatin A	HDAC	10 μg/ml	10 μg/ml	
AG825	HER2, EGFR	-	-	
Alendronate	HMG-CoA reductase	-	-	
Lovastatin	HMG-CoA reductase	-	-	
Risedronate	HMG-CoA reductase	-	-	
17-AAG	HSP90	-	-	
Herbimycin A	HSP90	-	-	T**
Radicicol	HSP90	-	-	T**
2-deoxyglucose	glycolysis	-	10 mM	*HIT*
1400W, HCl	iNOS	-	-	
AMT, HCl	iNOS	-	-	
Cucurbitacin I	Jak-2	0.3 μM	0.3 μM	

Compound		EC_{100}		
name	category	single	with MRI*	
Pifithrin-a (cyclic)	p53	-	-	
PRIMA-1	p53 activator	-	-	
Finasteride	5a-reductase	-	-	
Aminoglutethimide	aromatase	-	-	
Formestane	aromatase	-	-	
Mifepristone	progesterone receptor	-	-	
TOFA	acetyl-CoA carboxylase	-	-	
Amastatin	aminopeptidase A	-	-	
Actinonin	aminopeptidase M	-	-	
HA 14-1	Bcl-2	-	-	
BH3I-1	Bcl-XL	-	-	
LFM-A13	BTK	-	-	
Terreic acid	BTK	-	-	
E-64d	calpain	-	-	
ALLN	calpain, cathepsin B, L	-	-	
CA-074	cathepsin B	-	-	
Pepstatin A	cathepsin D	-	-	
Z-GLF-CMK	cathepsin G	-	-	
RS 102895	CCR2	-	-	
SB 328437	CCR3	-	-	
SB 225002	CXCR2	-	-	
AMD3100 - 8HCl	CXCR4	-	-	
NSC95397	Cdc25	-	-	
SC-ααα9	Cdc25A	-	-	
Amiloride	Na channel	-	-	
Lidocaine	Na channel	-	-	
Ouabain	Na/K ATPase	-	-	
Sanguinarine	Na/K/Mg ATPase	-	-	
Glibenclamide	K channel	-	-	
Dequalinium	K channel	-	-	
Diazoxide	K channel opener	-	-	
Inostamycin	PI turnover	1 μg/ml	1 μg/ml	
Nigericin	K ionophore	3 μM	3 μM	
Valinomycin	K ionophore	-	-	
Diltiazem	Ca channel	-	-	
Nifedipine	Ca channel	-	-	
Verapamil	Ca channel, MDR	-	-	
PGP-4008	MDR	-	-	
Fumitremorgin C	BCRP	-	-	
A23187	Ca ionophore	0.1 μM	0.1 μM	T**
Ionomycin	Ca ionophore	0.1 μM	0.1 μM	T**
t-Butylhydroquinone	Ca-ATPase	-	-	
Thapsigargin	SERCA	-	-	T**
N-phenylanthranilic acid	Cl channel	-	-	
DIDS	Cl channel	-	-	
SB 218078	Chk 1	-	-	
Debromohymenialdisine	Chk 1, 2	-	-	
Rotenone	mitochondrial complex I	-	-	
Antimycin A1	mitochondrial complex III	10 μg/ml	10 μg/ml	T**
Oligomycin	mitochondrial complex V	10 μg/ml	10 μg/ml	
R59022	DAG kinase	-	-	
Dioctanoylglycol	DAG kinase	-	-	
RHC80267	DAG lipase	-	-	
Xanthohumol	DAG acyltransferase	-	-	
C75	fatty acid synthase	-	-	

(continuing)